Supporting Information

Biofabrication of multifunctional nanocellulosic 3D structures: a facile and customizable route

Luiz G. Greca, Janika Lehtonen, Blaise L. Tardy, Jiaqi Guo, Orlando J. Rojas**

L. G. Greca[+], J. Lehtonen[+], Dr. B. L. Tardy[+], Dr. J. Guo, Prof. O. J. Rojas
Department of Bioproducts and Biosystems
School of Chemical Engineering
Aalto University
FI-00076 Aalto, Finland
E-mail: blaise.tardy@aalto.fi, orlando.rojas@aalto.fi
[+] These authors contributed equally to this work

Contents

Experimental section

Materials: Komagataeibacter medellinensis (former *Gluconacetobacter medellinensis*) was obtained from the

School of Engineering, Universidad Pontificia Bolivariana, Colombia and the properties of the strain have been reported elsewhere.[1] D-(+)–Glucose, yeast extract, peptone, sodium phosphate dibasic, citric acid, poly(ethylene glycol) (PEG) (average M_W 2 kDa), bovine serum albumin (BSA), chitosan, fluorescein isothiocyanate (FITC), FITC-dextran (average M_w 150 kDa), horseradish peroxidase (HRP), 2-methylimidazole, zinc acetate, sodium alginate, calcium chloride, gold (III) chloride hydrate ($HAuCl_4$), trisodium citrate, ethanol, acetone, sodium phosphate, hydrogen peroxide (30 % v:v in water) and poly(tetrafluoroethylene) (PTFE) powder (particle size 35 μm) were obtained from Sigma-Aldrich. Polystyrene particles (size 400 nm) were obtained from microparticles GMBH.

Synthesis of gold nanoparticles: $HAuCl_4$ solution (1 mM, 50 mL) was stirred vigorously and 1 % trisodium citrate (5 mL) was added rapidly when the solution boiled. A dark red colored solution was formed within several minutes and the colloidal solution was refluxed for an additional 30 min in order to ensure complete reduction. After cooling to room temperature, the colloidal particles were dialyzed in a regenerated cellulose membrane (MWCO 1 kDa) against deionized water for 3 days.

Synthesis of metal organic framework encapsulated enzyme (MOF-HRP): The protocol described by Liang et al. was closely followed.[2] Briefly, HRP (3 mg) was added into a solution of 2-methylimidazole (160 mM, 750 μL) in deionized water. The mixture was then mixed with a solution of zinc acetate dihydrate in deionized water (40 mM, 750 μL). The final mixture was left on a rotating mixer for 12 hours. The milky suspension was then washed by centrifugation two times with ethanol and then three times with water by successive isolation by centrifugation (Eppendorf Minispin, 9000 rpm, 2 min), replacement of the supernatant and resuspension.

Synthesis of FITC labelled Chitosan: Chitosan (medium M_W, ca. 250-300 kDa) (100 mg) was dissolved in Milli-Q water (25 mL) after addition of HCl (1M) to adjust the pH to 3. The solution was then adjusted to pH

6 and directly mixed with FITC (5 mg). After 2 hours the solution was returned to pH 3 and after another 2 hours the pH was neutralized to 7 and left overnight. The product was collected after dialysis in a regenerated cellulose membrane (MWCO 16 kDa) against, sequentially, diluted NaCl in dilued HCl and NaOH (< 1 mM) in ~ 5 L of deionized water to remove any unreacted excess dye. The dialysis exchange sequence was repeated three times. Finally, the solution was equilibrated against pH 3 (1 mM HCl) and further used for encapsulation.

Synthesis of FITC labelled BSA: BSA (30 mg) was dissolved in PBS buffer (12 mL, pH 7.2) and FITC in DMSO (1 mg mL^{-1}, 1.4 mL) was added. The solution was left in room temperature for 5 h in the dark under stirring. The product was collected after successive dialysis in a regenerated cellulose membrane (MWCO 16 kDa) against dilute NaCl solution to remove any excess dye.

Preparation of capsules and 3D shapes: K. medellinensis was incubated at 28 °C for 2 days in modified Hestrin-Schramm (HS) medium (80 mL, autoclaved, 121 °C, 20 min) before single drop-casting, spraying or molding. The medium was prepared by dissolving glucose (20 g L^{-1}), peptone (5g L^{-1}), yeast extract (5g L^{-1}) and Na_2HPO_4 (2.5 g L^{-1}) in Milli-Q water and the pH was adjusted to 4.5 with citric acid.

Drop-casting: Drops were dispensed with micropipettes at a given volume and rolled on a bed of autoclaved (121 °C, 20 min) PTFE powder until the apparent viscosity of the drop was considerably increased after which the drop was released. Drops were pipetted at 10, 20, 30, 40, 50 and 60 µl and incubated at 28 °C for given durations. The formed liquid marbles were kept in a humid environment during the incubation to prevent evaporation. After incubation, the formed bacterial cellulose (BC) capsules were immersed in deionized water to remove PTFE powder and purified in 0.1 M NaOH at room temperature for 24 h to remove bacteria and impurities remaining from the culture medium. The purified capsules were further washed with deionized water to remove the NaOH, and then stored in deionized water at 4 °C.

Spraying: The culture medium was rapidly sprayed to form drops onto a bed of PTFE powder until a considerable coverage with liquid marbles was observed. The sprayed drops were left for incubation for 3 days in a humid environment. The lower sizes obtained for capsules were delimited by the metal meshes used to separate the capsules from the stabilizing PTFE powder. In that manner capsules could be separated with sizes ranging between ca. 200 μm and 500 μm for the smallest fraction and between 500 μm and 3 mm for the larger fraction.

Molding: 3D shapes were produced from three different types of molds. For the customizable shapes, polylactic acid (PLA) molds were 3D-printed using the Ultimaker 2 Extended 3D-printer. For cuboids and cylinders, respectively, polystyrene (PS) rectangular molds (3000 μL, VWR International and a multiwell plate (300 μL, F96 MicroWell Plate VWR) were utilized. Eight-shaped and hexagonal commercial molds, produced by injection molding of poly(propylene) (PP), were also utilized.

Two different superhydrophobization approaches were developed to stabilize an air layer in between the mold and culture medium interface:

Method 1 - Partial dissolution of mold (principally used throughout the manuscript) - First, the molds were filled with acetone to ensure complete wetting of the internal surfaces. After ca. 30 seconds for PS and 5 min for PLA, excess acetone was removed, PTFE powder was rapidly added and the mold was closed to prevent complete solvent evaporation. By vigorous shaking of the mold, the PTFE powder uniformly covered and attached to all internal surfaces of the partially dissolved/swollen mold. Evaporation of the remaining solvent and removal of the excess PTFE powder resulted in an embedded layer of PTFE particles. The culture medium was then added into the superhydrophobized mold.

Method 2 - Liquid marbles transfer and coalescence - Seed liquid marbles (200 μL) were produced in a petri dish and transferred one by one (via pipetting) to the mold. Only a maximum of two marbles stayed inside of

the mold at the same time. After the marbles coalescence, by moving the pipette tip across their contacting interfaces, additional culture medium was added to compensate for the excess PTFE particles on the marble surface. The procedure was repeated until the desired volume was achieved.

The samples produced from PS and PLA molds were stabilized by the superhydrophobization method 1, while the samples produced from PP were stabilized by the method 2.

Bio welding: As a general procedure, 2 x 1 mL of culture medium were incubated separately inside superhydrophobized PS rectangular molds for 6 days. The rectangular molds were sealed with Parafilm to avoid the evaporation of the culture medium. Then, one cube was extracted to a container with deionized water, and readily transferred to the second rectangular mold with a pre-existing cube-shaped biofilm for another 6 days of incubation.

Permeability: Capsules were loaded with FITC-labelled dextran by immersion in a solution at a concentration of 10 mg mL^{-1} for 24 h. The capsules were then rapidly rinsed three times with water to remove excess dextran from the surface and then placed in Milli-Q water (1.2 mL) in an Eppendorf tube. The absorbance of the release medium was measured after defined times at 487 nm (Shimadzu UV-1800). The standard deviations were calculated based on the results from three samples.

Sodium alginate modification: The capsules loaded with FITC-dextran were immersed in sodium alginate solution (2 % (w:v)) for 30 min after the water rinse. No significant diffusion of dextran outside of the capsules was observed during immersion in alginate. This is potentially because the viscosity of the alginate solution was high. The capsules were then immersed in calcium chloride solution (3 % (w/v)) for 30 min, rinsed three times with water and placed in Milli-Q water (1.2 mL) and release of dextran was determined as described

previously.

Encapsulation: The culture medium was mixed 1:1 with a solution of 20% w:w of PEG of M_W 2 kDa for a final PEG concentration of 10% w:w. For drop-casting and spray preparation, a given amount of particles/cargo was added (between 5 and 25 µL of the cargo per 35 µL of culture medium–PEG mixtures) and thoroughly mixed until the particles were well suspended. Polystyrene particles, gold particles, FITC-chitosan, FITC-BSA and MOF-HRP concentrations were between ca. 5 and 0.5%. The capsules were then biofabricated during 2 days for all cargos except for FITC-chitosan (potentially because of bacterial growth hindrance of the polymer) and MOF-HRP where the higher pH required a biofabrication time of 4 days (see detailed description below). For the encapsulation of prefabricated capsules, a given amount of sprayed capsules contained in 30 µL of deionized water was drop-casted in the PTFE bed, followed by the addition of 30 µL of the culture medium. The biofabrication occurred over 2 days after which the multi-compartmentalized particles were collected.

Preparation of MOF-HRP loaded capsules: MOF-HRP are degrading in the natural pH of BC culture medium. Therefore, several pHs were tested to prevent degradation of the MOF architecture without hindering growth of the bacteria (pH 7.16, 6.85 and 6.6, Figure S13). Capsules loaded with MOF-HRP grown at pH 6.6 and below showed little to no activity whereas capsules loaded with MOH-HRP grown at pH 7.16 were feeble and deformed but had a significant activity. Capsules formed at pH 6.85 were robust and had a significant activity, therefore, this pH was chosen for biofabrication-based encapsulation.

Enzymatic assays of MOF-HRP loaded capsules: MOF-HRP loaded capsules were immersed in 3 mL of sodium phosphate buffer (50 mM, pH 7) and the baseline was measured. 20 µL of a stock solution of o-dianisidine (5 mg mL^{-1}) were then added. After mixing, 0,5 uL of hydrogen peroxide was added following by inversion mixing. The UV absorbance of the solution was then measured at given times and the absorbance at

440 nm was plotted against time. Three individual marbles were measured per curve and the average is reported.

Scanning Electron Microscopy: The capsules were frozen (-22 ˚C) and freeze-dried in a vacuum dryer (Labconco). Frozen capsules were fractured with a sharp blade for images of cross-section. Samples were mounted on aluminum stubs using double-sided carbon tape.

Before imaging, the freeze-dried BC samples and the superhydrophobized molds were sputter coated with a 3 nm layer of platinum-palladium alloy. The samples were examined using a field emission scanning electron microscope (FE-SEM) (Zeiss SigmaVP) operating at an acceleration voltage of 1.6 kV and a working distance of ca. 4 mm.

Mechanical analysis: Compression: Capsules of 20, 40 and 60 µL produced via drop casting were incubated for 4 days. The compression tests were done using a Dynamic Mechanical Analysis instrument (Q800 from TA instruments). The ramp force was set to 100 mN min^{-1}, until reaching a maximum of 5 mN.

Tensile: To analyze the effect of incubation time on the mechanical properties of the molded biofilms, 1.5 mL of the culture medium was incubated for 3, 5 or 7 days in superhydrophobized PS rectangular molds. To analyze the bio-welding strength, control samples of 2 mL were incubated during 12 days (same total time of incubation for bio-welded samples) and tested against standard biowelded samples. To limit deformation of the sample during clamping, prior to the tensile tests, all samples were compressed laterally to a thickness of 0.9 mm. A metallic plate of 0.9 mm was used in between the pressing plates as a spacer to yield a set final thickness of the biofabricated objects used for tensile testing. All tensile tests were performed with a universal tensile tester (Instron 4204 Universal Tensile Tester), with a loading rate of 20 mm min^{-1} and a distance in between clamps of 5 mm. For all conditions, the average values and the standard deviation were calculated based on at least three samples.

Gravimetric analysis: Capsules were freeze-dried as described earlier and weighed with an accuracy of 0.001 mg (Mettler Toledo MT5). For each volume and growth time, three capsules were analyzed and standard deviations were calculated based on the results. For the dry weight versus incubation time analysis (Figure 1d) the data was fitted by using the Hill1 growth function with Origin 2017 (version 94E).

UV-Vis spectroscopy: The UV-absorbance of the encapsulated samples was recorded by using a Shimadzu UV-2550 spectrophotometer (Shimadzu Corporation). All experiments were carried out at room temperature.

Bright Field Microscopy: Images were obtained on a Nikon Leica microscope in transmission mode. The camera was a JVC KY-F55BE with a resolution of 752×582.

Contact angle measurements: Contact angle images were taken utilizing the optical contact angle meter CAM 200 (KSV Instruments LTD) before and after superhydrophobization of PS and PLA molds.

Supplementary discussion

S1. Gravimetric analysis:

The rate of cellulose production in static cultures has been reported to be proportionally dependent on the surface area of the culture medium.[3] The thickness and yield of BC has been found to increase rapidly after few days and slow down after 7-10 days in static cultures.[4] In the confined volume approach used in this study, the maximum yield of BC was reached much faster as shown in Figure 1d. Figure S2a shows the glucose to cellulose yields from 4 days grown capsules. The highest yield of cellulose was achieved from the marble with an initial volume of 10 µL (3.5 g L^{-1}). This yield is similar to what has been reported with the same bacteria strain and carbon source and concentration as used in this study after 15 days in static culture.[5] This

suggests that the higher oxygen access enabled by the method used in this study increases growth rate and thus cellulose production. This is confirmed by slightly lower yields obtained from larger capsules, with a smaller surface area per volume. The effects of inoculation volume and concentration were not considered here.

S2. Molding:

The commercially available PS objects were chosen as molds because they are typically inexpensive, can be produced in large scale via injection molding, and are compatible with the partial mold dissolution as a superhydrophobization technique. From preliminary tests, the technique that provided the best results in terms of uniformity and oxygen access was the partial dissolution of the mold. With the liquid marble transfer and coalescence method, the 3D molded shapes often had imperfections due to the merging step, which often resulted in entrapment of PTFE powder inside of the molded capsules as can be seen in Figure S7d. For big molds (> 10 mL) and complex shapes, it became impractical.

S3. Bio-welding:

From optical microscopy (Figure 3), the biofilms were observed to have grown further not only in the direction of the interface with air, but also towards each other. Although the central part of the bio-welded interface is poorly supplied with oxygen, SEM image (Figure S10) showed the interaction between the networks of the two biofilms. Pulled out fibers are clearly seen in the interfacial area, denominated as region I in Figure S10, in contrast with the smoother outer surface, denominated as region III of the same SEM image.

S4. Permeability:

The permeability of BC membranes and the factors influencing it have been studied in several reports [6–8] and molecules such as lysozyme and bovine serum albumin have been shown to diffuse through a BC membrane [6] and the molecular-weight cutoff has been reported to be over 20 kDa.[8] In this study it was observed that

dextran with a molecular weight of 150 kDa can diffuse through the capsules.

The permeability of 40 µL capsules was studied by immersing capsules in FITC dextran solution and determining the release kinetics of the molecule from the capsule. Results of the release tests are shown in Figure S12. According to the results, incubation time did not affect permeability significantly, since there was no significant difference between the release from 1 day and 1 week grown capsules. The effect of removal of bacteria and adsorbed culture medium ingredients with NaOH on the release was also investigated. When the capsules were not treated with NaOH the release rate slightly slowed down indicating that the capsules are less permeable without the NaOH treatment. To slow down the release of FITC-dextran more efficiently, the capsules were modified with sodium alginate since this has earlier been reported to produce denser BC membranes.[9] Treatment of the capsules with sodium alginate solution followed by calcium chloride for crosslinking resulted in a significant decrease in the permeabilility of the capsules.

S5. Encapsulation:

a - Whereas FITC-BSA (ca. 66 kDa) was assumed to associate with the cellulosic capsules from adsorption of the protein onto the shell material (Figure S12a), when FITC-chitosan was encapsulated a clear distinction between the shell material and the cargo could be made suggesting that the polymer was not fully dissolved in growth conditions. Furthermore, the color was pH-responsive (Figure S12b) as the adsorption peak clearly changed as a function of pH (Figure S12b).

b - Gold nanoparticles synergize well with the thermal resistance of the biofabricated objects because of their potential use for plasmonic heating.[10] The fact that the capsules are chemically[11] and, more importantly, thermally stable,[12] make them an excellent candidate for such applications. Gold particles were succesfully loaded using the spray or the single drop-cast methodologies but had a significant interaction with the shell shifting their plasmonic absorbance (Figure S14c). For gold nanoparticles an important avenue that could be explored is their easy functionalization with steric layers of PEG preventing their aggregation and adhesion to

other interfaces. This improved colloidal stability by functionalization has been extensively studied and could easily be applied herein.[13,14]

Although not fully explored herein, the pH responsive behavior of FITC-chitosan cargo as well as the plasmonic response of gold particles encapsulated in biofabricated objects suggests their usefor sensing applications or plasmonic heating.

Supplementary Figures

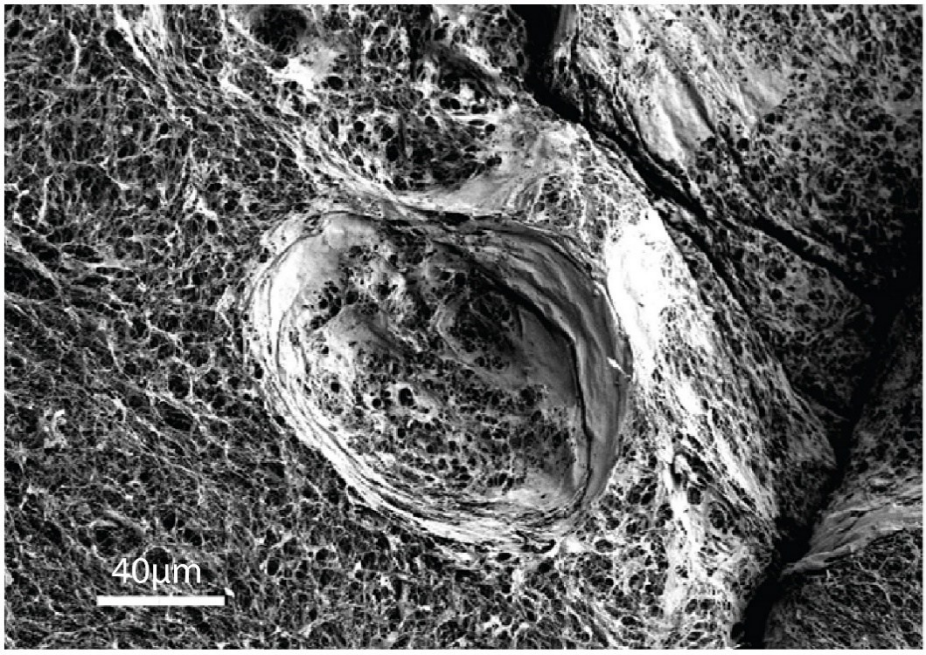

Figure S1. SEM image of a BC capsule surface fabricated by drop-casting showing micro imprint from PTFE particle.

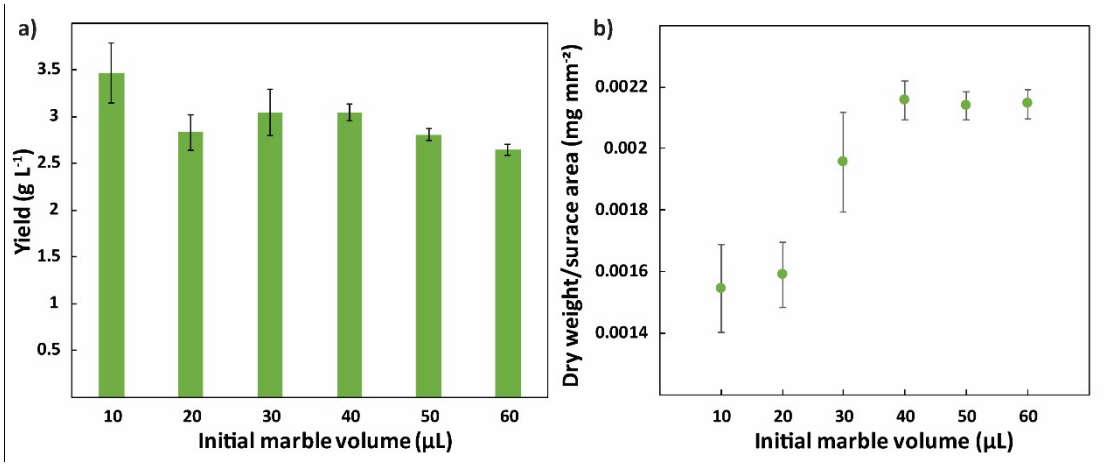

Figure S2. a) Yield as a function of initial marble volume for 4 days grown drop-cast marbles. b) Dry weight to surface area ratio plotted as a function of initial marble volume for 4 days grown marbles.

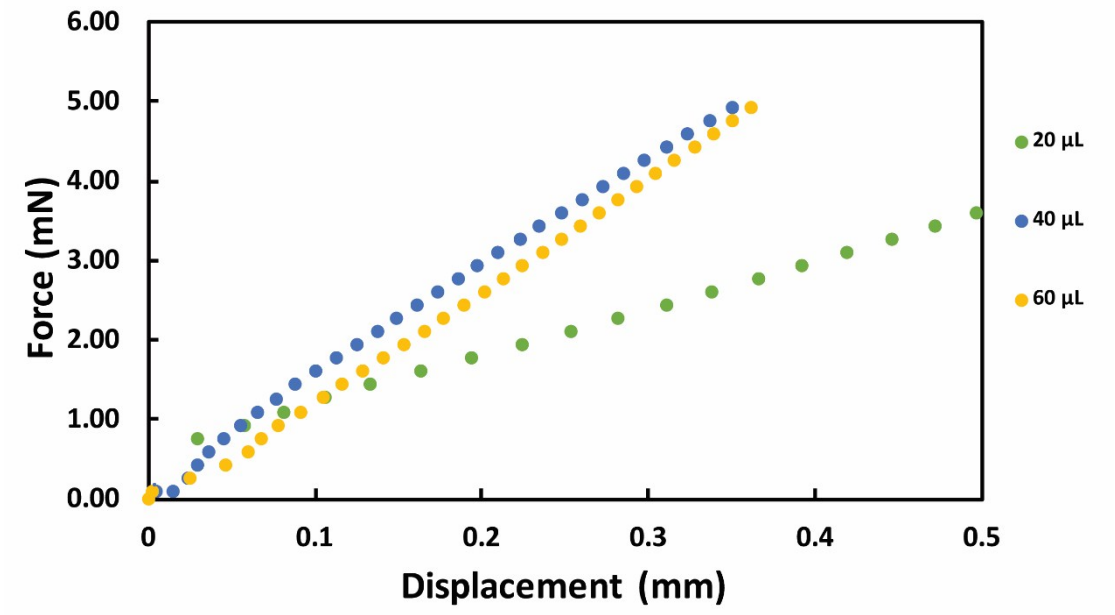

Figure S3. Force versus displacement data from dynamic mechanical analysis (compression) of BC capsules formed by drop-casting from initial volumes of 20, 40 and 60 µL.

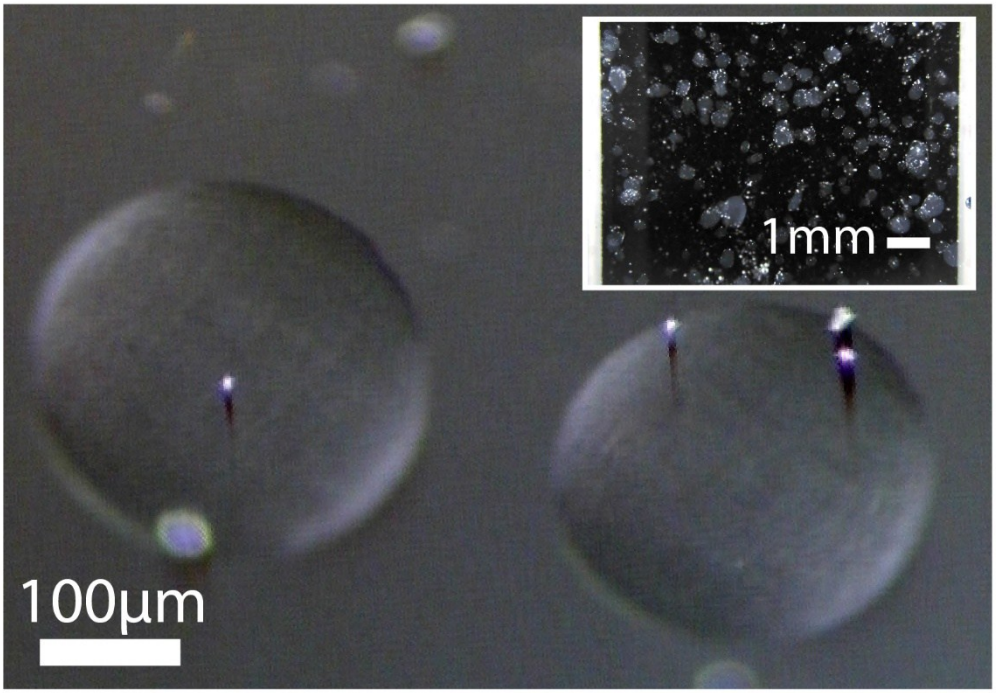

Figure S4. Capsules and (inset) suspensions of capsules obtained by the spraying methodology. Scale bar are 100 µm and 1 mm.

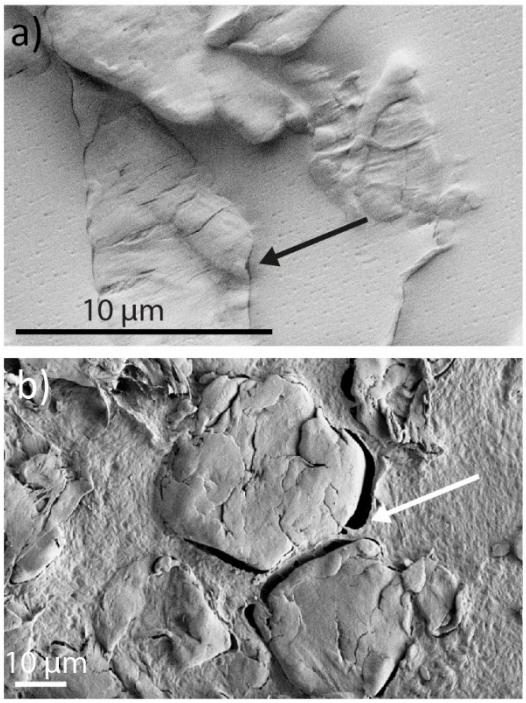

Figure S5. SEM image of superhydrophobized a) polystyrene and b) PLA surfaces showing entrapment of PTFE particles. Arrows indicate discontinuities highlighting that the entrapment is due to a mechanical locking rather than compatibilization with the polymer matrix of the mold.

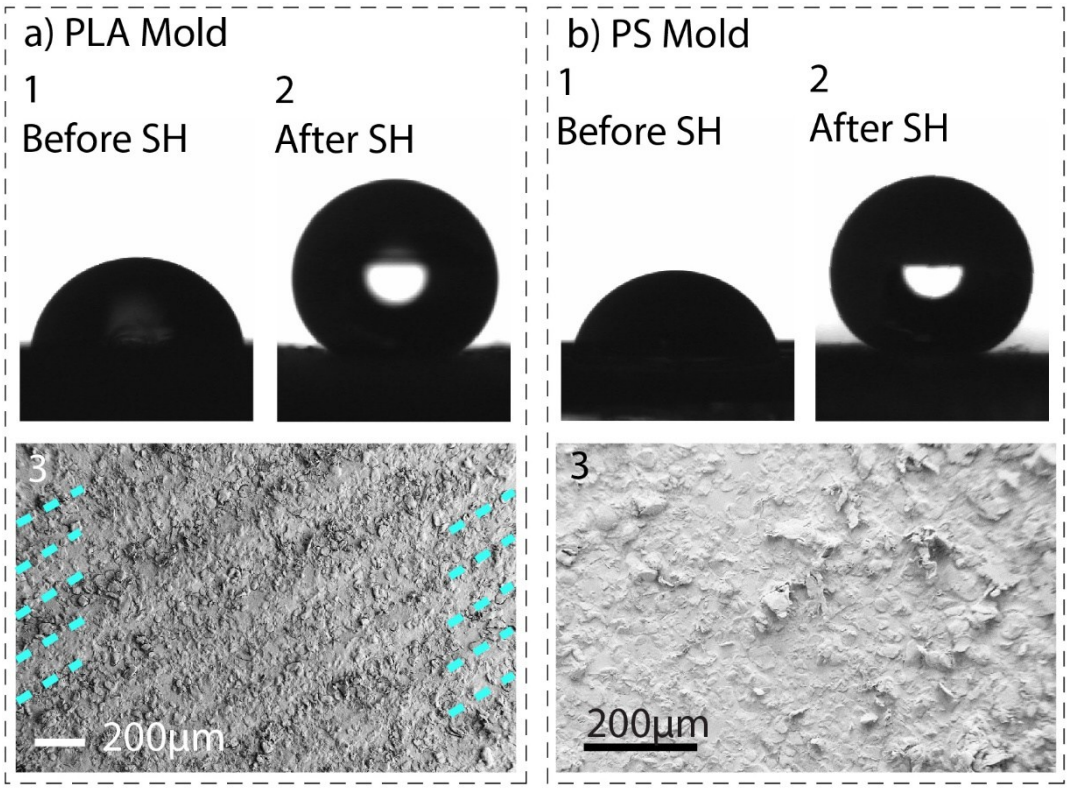

Figure S6. Contact angles of water against the polymeric molds and SEM of their surfaces. a) 3D-printed PLA mold (1) before and (2) after superhydrophobization. (3) SEM of the superhydrophobized PLA mold surface. Dashed blue lines highlight the topographical features resulting from the 3D printing process b) commercial injection-molded PS mold (1) before and (2) after superhydrophobization. (3) SEM of the superhydrophobized PS mold surface.

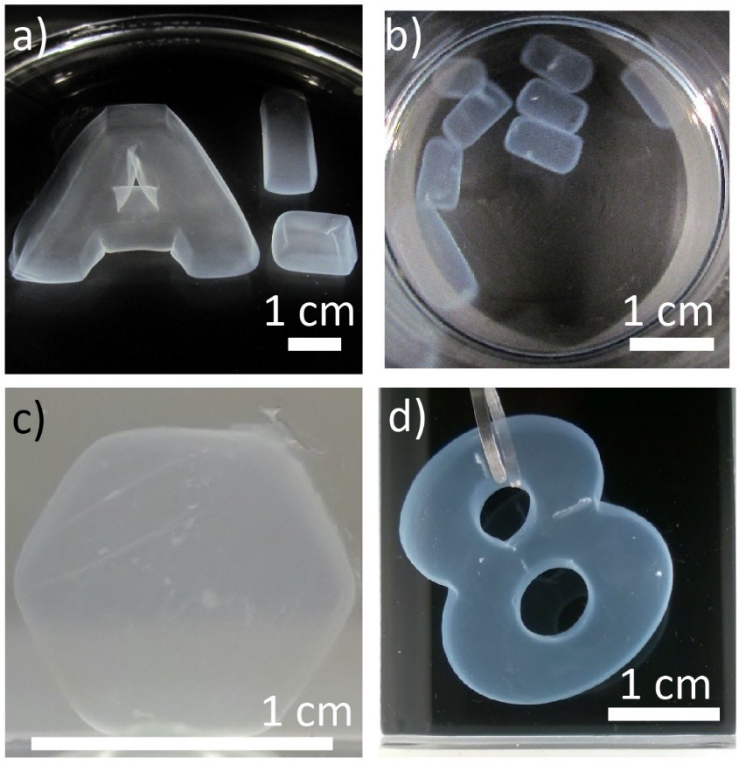

Figure S7. Additional examples of 3D objects biofabricated by using the molding methodology. a) "A" shape and b) cylindrical objects obtained by using superhydrophobized 3D printed PLA mold and injection molded mold respectively. c), d) Hexagonal and eight shapes obtained by using polypropylene molds and the liquid-marble transfer and coalescence method.

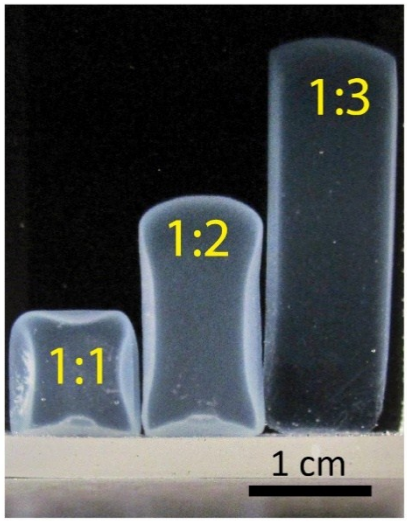

Figure S8. Cuboids of different aspect ratios formed by casting different amounts of culture medium to

superhydrophobized polystyrene rectangular molds.

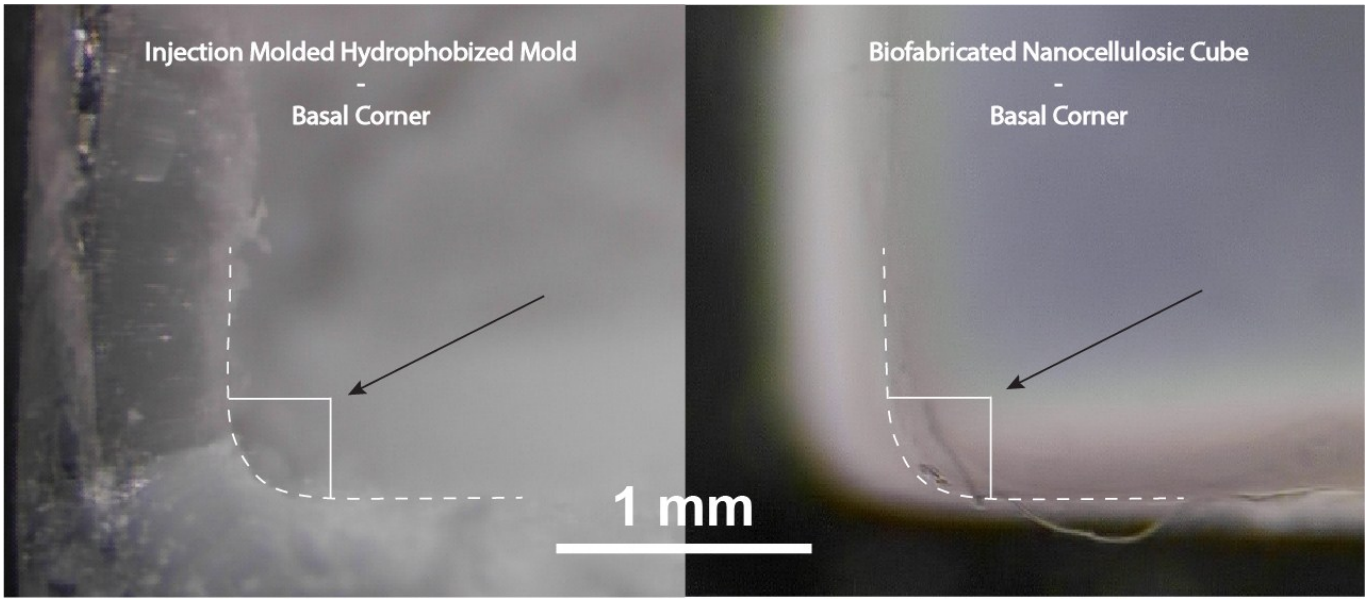

Figure S9. Micrographs obtained by brightfield microscopy comparing the basal piece of a superhydrophobized injection molded molds (left) with the replica obtained by biofabrication (right).

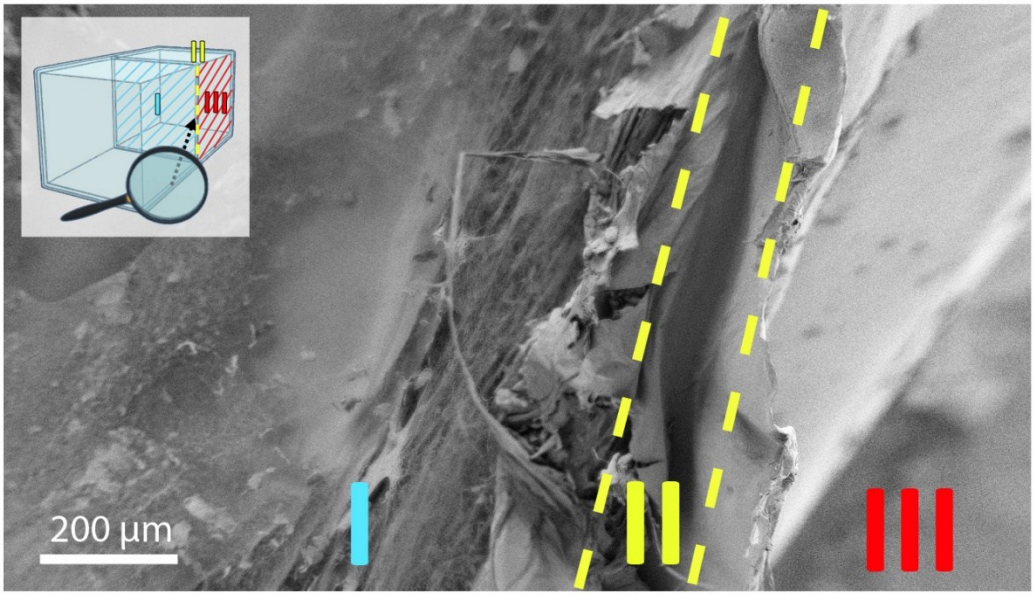

Figure S10. SEM image of a freeze-dried bio-welded sample after fracture. I represents the top view of the bio-welded interface, II is the welded area where both cubes were joined that was exposed to the air-water

interface during welding, and III is the external face of one of the bio-welded cubes.

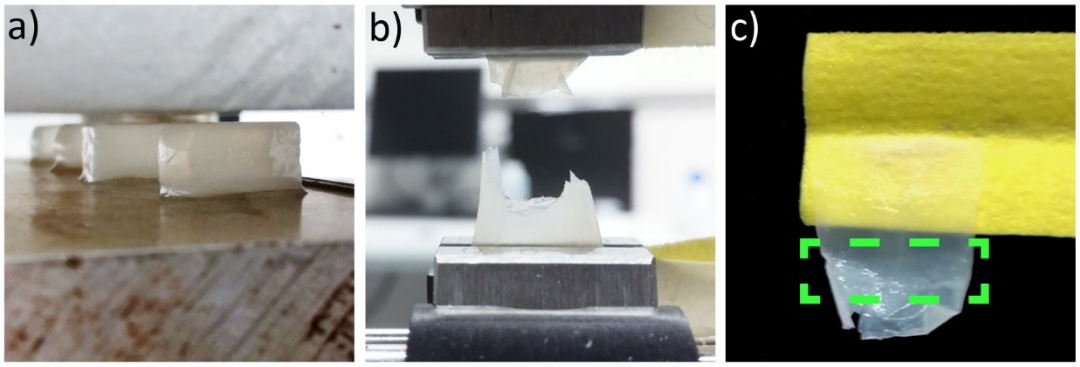

Figure S11. Tensile testing of biowelded cubes biofabricated in superhydrophobized rectangular molds. a) Compression of the biowelded samples prior to tensile test to prevent deformation during clamping. b) Fracture in the mid-section of biowelded cubes after tensile testing. c) Biowelded sample after tensile test, indicating that breakage did not occur at biowelded region.

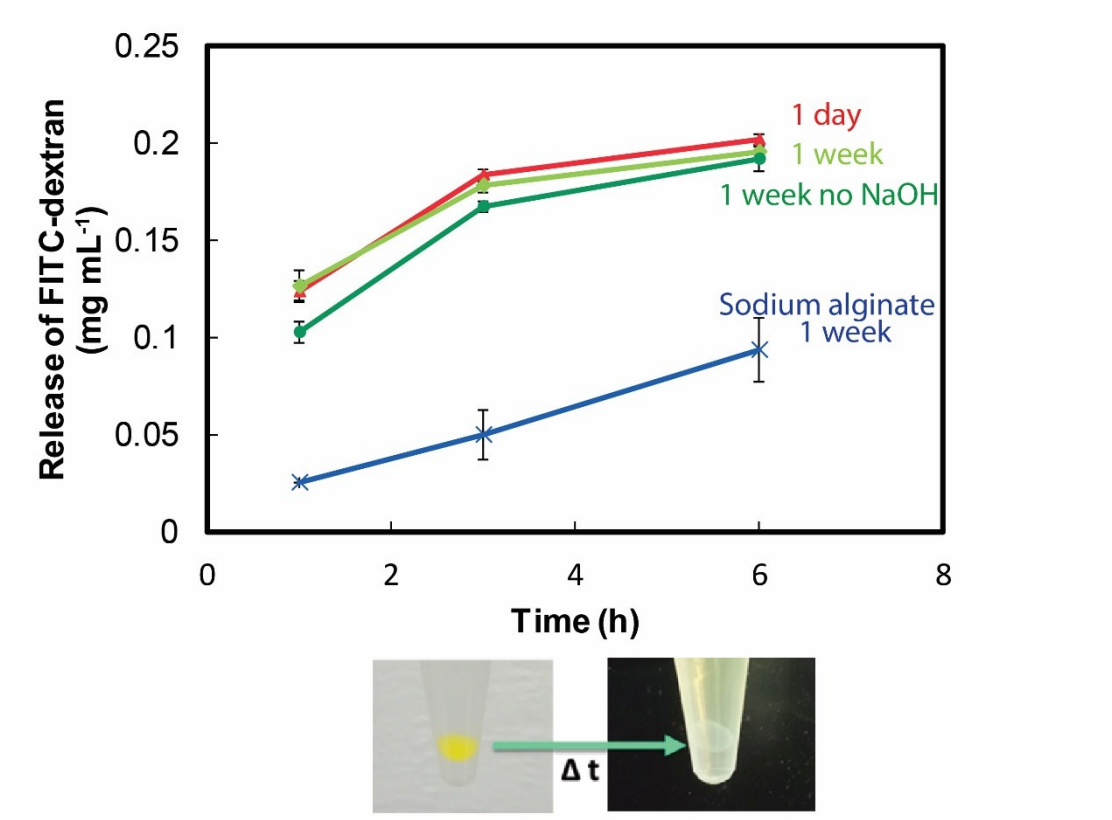

Figure S12. Release of FITC-dextran (molecular weight 150 kDa) from drop-casted based biofabricated 40 µL

capsules grown 1 day or 1 week (with and without NaOH purification) and 1 week grown capsule with post modification with sodium alginate. Note that the total amount of loaded FITC-dextran may have been reduced from the crosslinking step (see experimental).

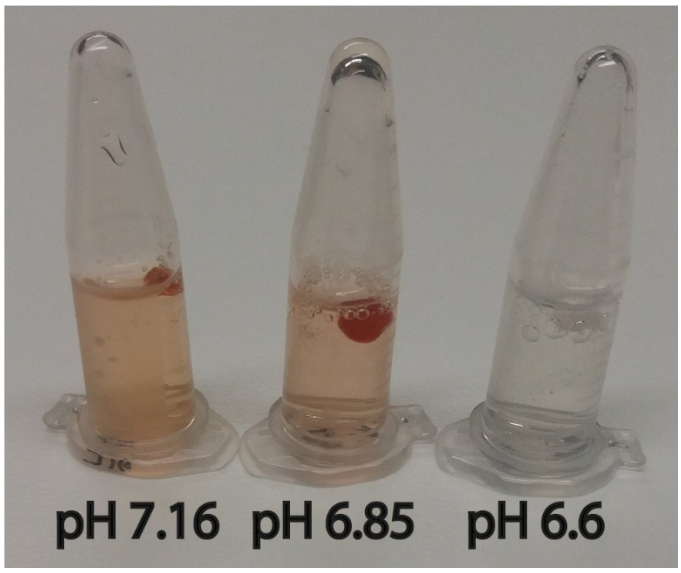

Figure S13. Effect of culture medium growth condition on activity of the encapsulated metal organic framework encapsulated horseradish peroxidase. For BC capsules grown at pH 7.16 the activity is considerable but the formation of the shell is hindered and the resulting capsule is deformed and unstable. For BC capsules grown at pH 6.6 although the shell is intact no activity from the enzyme is observed whereas. For BC capsules grown at pH 6.85 the capsules replicated closely the drop-cast liquid marble morphology and a high activity of the enzyme is observed.

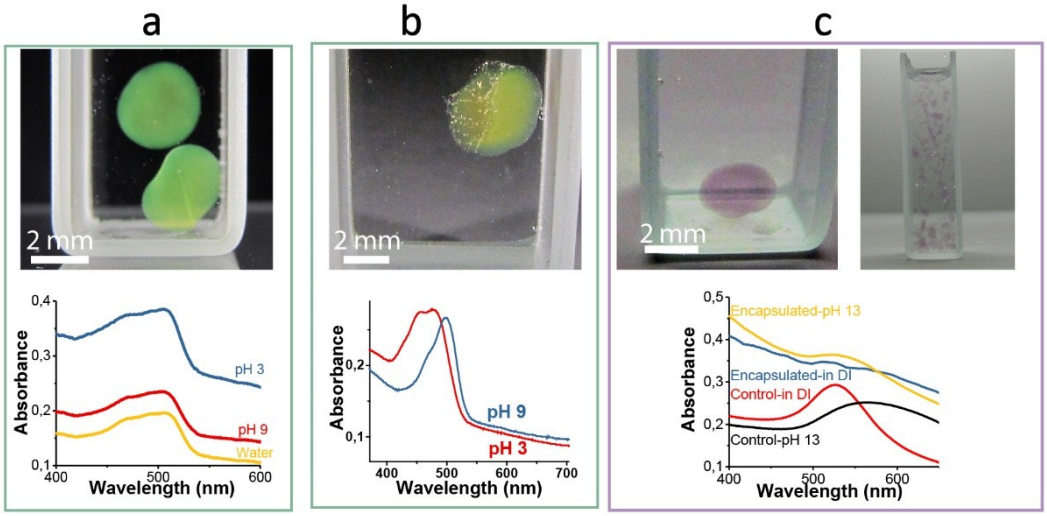

Figure S14. Encapsulation of various cargo. a) Capsules with FITC-BSA as cargo, indicating that BSA is on the BC shell b) Capsules with FITC-chitosan as cargo, indicating that chitosan is encapsulated. c) Gold nanoparticles. For all encapsulated systems corresponding UV-Vis absorbance as a function of pH are shown below. For the gold particles the plasmonic response of the pure suspension is shown as a function of pH (control) and highlights a high adhesion of the nanoparticles on the shell of the BC capsules.

Supplementary references

[1] C. Castro, R. Zuluaga, C. Álvarez, J. L. Putaux, G. Caro, O. J. Rojas, I. Mondragon, P. Gañán, *Carbohydr. Polym.* **2012**, *89*, 1033.

[2] K. Liang, R. Ricco, C. M. Doherty, M. J. Styles, S. Bell, N. Kirby, S. Mudie, D. Haylock, A. J. Hill, C. J. Doonan, P. Falcaro, *Nat. Commun.* **2015**, *6*, 7240.

[3] S. Masaoka, T. Ohe, N. Sakota, *J. Ferment. Bioeng.* **1993**, *75*, 18.

[4] M. Iguchi, S. Yamanaka, a. Budhiono, *J. Mater. Sci.* **2000**, *35*, 261.

[5] C. Molina-Ramírez, M. Castro, M. Osorio, M. Torres-Taborda, B. Gómez, R. Zuluaga, C. Gómez, P. Gañán, O. J. Rojas, C. Castro, *Materials (Basel).* **2017**, *10*, DOI 10.3390/ma10060639.

[6] A. M. Sokolnicki, R. J. Fisher, T. P. Harrah, D. L. Kaplan, *J. Memb. Sci.* **2006**, *272*, 15.

[7] M. Park, S. Shin, J. Cheng, J. Hyun, *Carbohydr. Polym.* **2017**, *158*, 133.

[8] H. Shibazaki, S. Kuga, F. Onabe, M. Usuda, *J. Appl. Polym. Sci.* **1993**, *50*, 965.

[9] T. Suratago, S. Taokaew, N. Kanjanamosit, K. Kanjanaprapakul, V. Burapatana, M. Phisalaphong, *J. Ind. Eng. Chem.* **2015**, *32*, 305.

[10] O. Neumann, A. S. Urban, J. Day, S. Lal, P. Nordlander, N. J. Halas, *ACS Nano* **2013**, *7*, 42.

[11] T. Liebert, *Cellul. Solvents Anal. Shap. Chem. Modif.* **2010**, 3.

[12] J. George, K. V. Ramana, A. S. Bawa, Siddaramaiah, *Int. J. Biol. Macromol.* **2011**, *48*, 50.

[13] J. Gao, X. Huang, H. Liu, F. Zan, J. Ren, *Langmuir* **2012**, *28*, 4464.

[14] W. Fu, D. Shenoy, J. Li, C. Crasto, G. Jones, C. Dimarzio, S. Sridhar, M. Amiji, *MRS Proc.* **2004**, *845*, 1.